Influence of shape and energy anisotropies on the phase diagram of discotic molecules

D. Caprion,[1] L. Bellier-Castella,[2,*] and J.-P. Ryckaert[1]
[1]*Physique des Polymères, Université Libre de Bruxelles, Campus Plaine, Case Postale 223, B-1050 Brussels, Belgium*
[2]*Département de Physique des Matériaux (UMR 5586 du CNRS), Université Claude Bernard-Lyon 1, 69622 Villeurbanne Cedex, France*
(Received 22 January 2003; published 11 April 2003)

We present Monte Carlo simulations of discotic molecules using the Gay-Berne potential with shape (κ) and energy (κ') anisotropies. Following the previous work of Bates and Luckhurst [J. Chem. Phys. **104**, 6696 (1996)] at $\kappa=0.345$, $\kappa'=0.2$ when we determine the sequence of different phases at the same reduced pressure $P^*=50$, we find an additional phase at low temperatures corresponding to an orthorhombic crystalline phase and we characterize it. Keeping the shape anisotropy fixed at $\kappa=0.2$, we determine the evolution of the phase diagram with varying energy anisotropy. At high κ', low anisotropy, the system is not able to build columns while at low κ', the system exhibits both orthorhombic crystal as well as hexagonal liquid crystal phases over a wide range of pressures and temperatures. The domain of stability of the nematic phase is found to systematically shift towards higher pressures as κ' decreases.

DOI: 10.1103/PhysRevE.67.041703 PACS number(s): 64.70.Md, 61.20.Ja, 83.80.Xz

I. INTRODUCTION

Liquid crystals are now common materials present in numerous devices such as computer screens or watches. They are generally composed of elongated rodlike molecules. However, since the late 1970s, when they were first synthesized [1], the family of disk-shaped liquid crystal molecules is growing rapidly. Such discotic molecules have been proposed for use in xerography [2] and as chemical sensors [3] for instance.

As with the rodlike molecules, the discotic molecules exhibit a rich phase diagram depending on temperature. They show an isotropic phase *I* at high temperature neither with any orientational nor long-range positional order. On decreasing the temperature, the molecules align on an average along a common direction, and form the so-called nematic phase *N*. On further decreasing the temperature, one observes a specific phase, the columnar phase (Col), in which the molecules are stacked on top of each other to form columns. These columns present a long-range two-dimensional (2D) order in the orthogonal plane, while the order along their axis is at least partially liquidlike. The symmetry in the plane perpendicular to the columns can be hexagonal (Col_h) or rectangular (Col_r) (see, for instance, Ref. [4]).

The sequence of phases *I*-*N*-Col is observed experimentally like for some benzoate esters of triphenylene which show an *I*-*N*-Col_r sequence. However, other discotic molecules only exhibit an *I*-Col_r or *I*-*N* sequence of transitions [5–7]. Discotic molecules are composed of an aromatic core (i.e., rigid and flat) on which flexible chains are added in the equatorial plane. The length and/or the composition of these chains have been observed to play an important role for the existence (or not) of a nematic or columnar phase. One should also notice that these sequences are generally obtained at atmospheric pressure, studies at higher pressure being very limited so far [8–10].

From simulation and theory, only a few determinations of phase diagrams have been attempted. Thin hard platelets [11], hard oblate ellipsoids [12,13], and cut hard spheres show nematic and isotropic phases, but only the last one shows a columnar phase [14]. Models describing anisotropic particles with continuous attractive and repulsive interactions such as described by the Gay-Berne potential [15] show *I*, *N*, Col, as well as crystalline (Cr) phases, depending on the pressure [16–18]. Moreover, a recent study [19] based on density-functional theory presents the phase diagram for one of the latter models, and its evolution with the model parameters such as the shape anisotropy. Although many Monte Carlo simulations have been carried out to study the influence on the phase diagram of the shape or of the anisotropy of the attractive interaction between rodlike molecules [20], to our knowledge no systematic study of the influence of the shape or/and of the interactions has been performed for discotic molecules.

The aim of the present work is therefore to study the influence of the shape and the energy anisotropies on the phase diagram of a system of discotic molecules. For that purpose, we use the well known Gay-Berne potential characterized by a shape anisotropy parameter $\kappa<1$ representing the thickness over diameter ratio and an energy anisotropy parameter κ' which is the ratio of the edge-to-edge energy minimum over the face-to-face energy minimum. It has been shown [17] that with the pair of values $\kappa=0.345$ and $\kappa'=0.2$, when the temperature is reduced progressively, the system evolves successively from an *I* to an *N* and then to a Col phase. In the present study, we look at the changes in the phase diagram as κ' is varied, keeping the shape anisotropy unchanged and equal to $\kappa=0.2$, a value justified by the actual shape of many discotic molecules.

Our model and some simulation details are gathered in Sec. II. Our results, presented in Sec. III, are divided into two parts. First, using the set of parameters of Bates and Luckhurst for a preliminary test, we follow an isobar for quite a large system of $N\approx 2200$ discotic molecules and find the expected phase transitions, and in addition, at lower temperature, a crystal phase which we characterize in detail. In the

*Present address: Commissariat à l'Energie Atomique, DAM Ile de France, DPTA BP12, 91680 Bruyères-le-Chatel, France.

second part of Sec. III, we follow the evolution of the phase diagram as the energy anisotropy varies, while the thickness over diameter ratio is fixed at 0.2. Section IV summarizes our conclusions about the domain of the κ, κ' parameters for which the columnar phase is stable.

II. SIMULATIONS

A. Model

To model the interactions between discotic molecules, we choose a simple, but efficient, pairwise additive potential, namely, the Gay-Berne potential [15]. The latter has been successfully used in several previous studies to reproduce either nematic, smectic, or columnar phases [15–17,20–26]. It can be written as follows [17]:

$$U_{ij}(\hat{\mathbf{u}}_i,\hat{\mathbf{u}}_j,\mathbf{r}_{ij}) = 4\mathcal{E}(\hat{\mathbf{u}}_i,\hat{\mathbf{u}}_j,\hat{\mathbf{r}}_{ij})\left[\left(\frac{\sigma_{ff}}{r_{ij}-\sigma(\hat{\mathbf{u}}_i,\hat{\mathbf{u}}_j,\hat{\mathbf{r}}_{ij})+\sigma_{ff}}\right)^{12} - \left(\frac{\sigma_{ff}}{r_{ij}-\sigma(\hat{\mathbf{u}}_i,\hat{\mathbf{u}}_j,\hat{\mathbf{r}}_{ij})+\sigma_{ff}}\right)^{6}\right], \quad (1)$$

where the unit vectors $\hat{\mathbf{u}}_i$ and $\hat{\mathbf{u}}_j$ define the orientation of the two interacting molecules and σ_{ff} their thickness.

The effective energy is given by

$$\mathcal{E}(\hat{\mathbf{u}}_i,\hat{\mathbf{u}}_j,\hat{\mathbf{r}}_{ij}) = \mathcal{E}_0\mathcal{E}_1^{\nu}(\hat{\mathbf{u}}_i,\hat{\mathbf{u}}_j)\mathcal{E}_2^{\mu}(\hat{\mathbf{u}}_i,\hat{\mathbf{u}}_j,\hat{\mathbf{r}}_{ij}), \quad (2)$$

with

$$\mathcal{E}_1 = [1-\chi^2(\hat{\mathbf{u}}_i\cdot\hat{\mathbf{u}}_j)]^{-1/2}, \quad (3)$$

and

$$\mathcal{E}_2 = 1-\frac{\chi'}{2}\left(\frac{(\hat{\mathbf{u}}_i\cdot\hat{\mathbf{r}}_{ij}+\hat{\mathbf{u}}_j\cdot\hat{\mathbf{r}}_{ij})^2}{1+\chi'(\hat{\mathbf{u}}_i\cdot\hat{\mathbf{u}}_j)}+\frac{(\hat{\mathbf{u}}_i\cdot\hat{\mathbf{r}}_{ij}-\hat{\mathbf{u}}_j\cdot\hat{\mathbf{r}}_{ij})^2}{1-\chi'(\hat{\mathbf{u}}_i\cdot\hat{\mathbf{u}}_j)}\right). \quad (4)$$

The effective radius $\sigma(\hat{\mathbf{u}}_i,\hat{\mathbf{u}}_j,\hat{\mathbf{r}}_{ij})$ is expressed as

$$\sigma(\hat{\mathbf{u}}_i,\hat{\mathbf{u}}_j,\hat{\mathbf{r}}_{ij}) = \sigma_0\left[1-\frac{\chi}{2}\left(\frac{(\hat{\mathbf{u}}_i\cdot\hat{\mathbf{r}}_{ij}+\hat{\mathbf{u}}_j\cdot\hat{\mathbf{r}}_{ij})^2}{1+\chi(\hat{\mathbf{u}}_i\cdot\hat{\mathbf{u}}_j)} + \frac{(\hat{\mathbf{u}}_i\cdot\hat{\mathbf{r}}_{ij}-\hat{\mathbf{u}}_j\cdot\hat{\mathbf{r}}_{ij})^2}{1-\chi(\hat{\mathbf{u}}_i\cdot\hat{\mathbf{u}}_j)}\right)\right]^{-1/2}. \quad (5)$$

In the expressions (2) and (5), $\mathcal{E}_0$ and σ_0 are the energy and length scales.

Both the effective energy $\mathcal{E}$ and the effective radius σ depend on the intermediate parameters χ and χ' and on the *ad hoc* exponents μ and ν. χ and χ' can be expressed in terms of the shape and energy anisotropy ratios κ and κ'. They are respectively defined as

$$\chi = \frac{\kappa^2-1}{\kappa^2+1} \quad (6)$$

and

$$\chi' = \frac{\kappa'^{1/\mu}-1}{\kappa'^{1/\mu}+1}. \quad (7)$$

Using common definitions, we have $\kappa=\sigma_{ff}/\sigma_{ee}$ and $\kappa'=\mathcal{E}_{ee}/\mathcal{E}_{ff}$, where *ff* denotes the face-to-face configuration ($\hat{\mathbf{u}}_i\cdot\hat{\mathbf{u}}_j=1$ and $\hat{\mathbf{u}}_i\cdot\hat{\mathbf{r}}_{ij}=1$), while *ee* is the edge-to-edge one ($\hat{\mathbf{u}}_i\cdot\hat{\mathbf{u}}_j=1$ but $\hat{\mathbf{u}}_i\cdot\hat{\mathbf{r}}_{ij}=0$). We can still define two other typical configurations: the *T* configuration ($\hat{\mathbf{u}}_i\cdot\hat{\mathbf{u}}_j=0$, $\hat{\mathbf{u}}_i\cdot\mathbf{r}_{ij}=0$, and $\hat{\mathbf{u}}_j\cdot\hat{\mathbf{r}}_{ij}=1$) and the cross configuration ($\hat{\mathbf{u}}_i\cdot\hat{\mathbf{u}}_j=0$, $\hat{\mathbf{u}}_i\cdot\hat{\mathbf{r}}_{ij}=0$, but $\hat{\mathbf{u}}_j\cdot\hat{\mathbf{r}}_{ij}=0$). We note that the energy and distance units, $\mathcal{E}_0$ and σ_0, correspond to the potential energy minimum and the distance for which the potential is zero in the cross configuration, respectively, while σ_0 also corresponds to σ_{ee}.

In this work, we fix the values of μ and ν to 1 and 2, respectively, and cut the potential for distances greater than $1.6\sigma_{ee}$, following the previous choice of Bates and Luckhurst [17]. We express the physical quantities in reduced unit, e.g., distances $r^*=r/\sigma_{ee}$, pressures $P^*=P\sigma_{ee}^3/\mathcal{E}_0$, temperatures $T^*=k_BT/\mathcal{E}_0$, and enthalpy $H^*=H/\mathcal{E}_0$.

B. Procedure

We perform Monte Carlo (MC) simulations of 2197 discotics enclosed in a parallelepipedic box with periodic boundary conditions. These simulations are performed in the *N-P-T* ensemble to avoid the cavitation effect observed by Emerson *et al.* [16]. For each thermodynamic point (P^*, T^*), we first equilibrate the system for 50 000 MC cycles (MCCs), when the system is far from a transition, and for 200 000 MCCs when it is close to a transition. The length of the measurements depends on the desired properties: typically 20 000 MCCs for thermodynamic and structural quantities, and up to 150 000 MCCs for diffusional quantities. A MC cycle consists of, in average, one trial movement (rotational or translational) for each discotic molecule, and one box length trial change. The box edges are treated independently to ease transitions, especially the isotropic-nematic one, by nonisotropic contractions of the box. We start the simulations from high temperatures, in the isotropic phase and decrease the temperature (keeping the pressure constant) by steps of $\Delta T^*=0.2$. Close to the phase transition points, some additional runs are performed with a smaller decrease ($\Delta T^*=0.05$) to locate the transitions with more precision. We also run some simulations starting from a low temperature (typically $T^*=0.2$) to determine the hysteresis and to confirm the assumptions on the symmetry of the low temperature phase (see below).

III. RESULTS AND DISCUSSION

To start this study, we choose to use as reference the parameter set investigated by Bates and Luckhurst [17], where κ and κ' are taken equal to 0.345 and 0.2, respectively. The choice of these values is based on previous simulations [16], molecular mechanics, and energetics calculations [17]. This choice of parameters leads to the formation of nematic and columnar phases depending on pressure and temperature.

In a second step, we fix the value of κ at 0.2 and let that of κ' vary from 0.8 to 0.1. This covers a set of situations ranging from weak to strong face-to-face attractions.

A. The $\kappa=0.345$ and $\kappa'=0.2$ case

We first recalculate the phase diagram of the Gay-Berne model with the Bates and Luckhurst parameters on a system of $N=2197$ discotics.

In agreement with the previous study [17], we find three phases depending on pressure and temperature. To determine the phase transitions, we monitor physical quantities such as enthalpy, volume, or the second-rank orientational order parameter $\langle P_2 \rangle$. This latter is obtained from diagonalization of the **Q** tensor defined as follows [11]:

$$Q_{\alpha\beta}=\frac{1}{2N}\sum_{i=1}^{N}(3u_{\alpha}^{i}u_{\beta}^{i}-\delta_{\alpha\beta}). \tag{8}$$

$\langle P_2 \rangle$ tends to zero in the isotropic phases (it is strictly equal to zero for an infinite sample). It is equal to about 0.6 in the nematic phase and to 0.8 in the columnar phase, see, for instance, Ref. [17].

At $P^*=50$, the following transition temperatures are found: $T^*_{I\text{-}N}=3.30\pm0.10$ and $T^*_{N\text{-}\mathrm{Col}_h}=2.90\pm0.10$. These values are in good agreement with the ones found earlier. We also compute the slope of the transition line dP^*/dT^* according to Clapeyron's law

$$\frac{dP^*}{dT^*}=\frac{1}{T^*}\frac{\Delta H^*}{\Delta V^*}. \tag{9}$$

We find 35.0 ± 4.5 and 60.5 ± 7.6 for the isotropic-nematic phase boundary and the nematic-columnar phase boundary, respectively. Bates and Luckhurst found 35.5 ± 2.0 and 52.2 ± 4.0, values which are also in fair agreement with our results.

To check the spatial packing of the different phases found during cooling, we also calculate the perpendicular radial distribution (PRD) function defined as

$$g_p(r)=\frac{V}{N^2 2\pi r h}\left\langle \sum_i \sum_{j\neq i} \delta(r-r_{ij}^{p})\right\rangle, \tag{10}$$

where V is the volume of the simulation box, N the number of discotics, and r_{ij}^{p} the perpendicular distance between discotic molecules i and j defined as $|\mathbf{r}_{ij}-(\mathbf{r}_{ij}\cdot\hat{\mathbf{u}}_i)\hat{\mathbf{u}}_i|$. For a given discotic molecule i, we limit the sum over all discotic molecules j so that the distance $|\mathbf{r}_{ij}\cdot\hat{\mathbf{u}}_i|$ is inferior or equal to h. We take in this study h equal to σ_{ff}.

In Fig. 1, we show the PRD below and above the N-Col$_h$ transition line. As the system crosses this line (from high temperatures), the discotic molecule positions are more and more ordered. This can be seen in the appearance of peaks at intermediate distances (greater than σ_{ee}) as the temperature decreases. At intermediate temperature ($T^*=2.80$), three broad peaks are observable for distances smaller than $2\sigma_{ee}$, they correspond to a hexagonal packing of the discotic molecules in the plane perpendicular to the columns with the typical positional ratio $1:\sqrt{3}:2$.

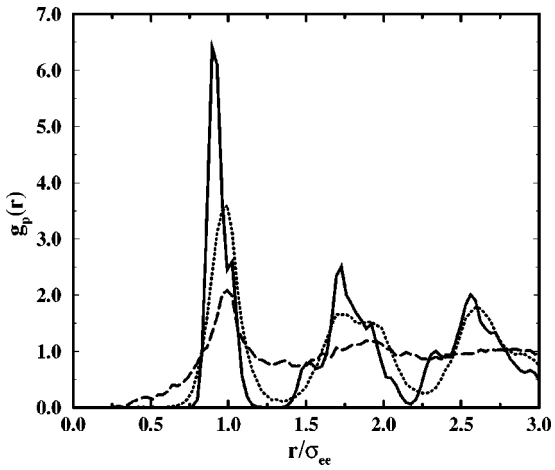

FIG. 1. Perpendicular radial distribution (see text for definition) for three different temperatures: $T^*=3.20$ (N) (long dashed), $T^*=2.80$ (Col$_h$) (dotted), and $T^*=1.40$ (Cr) (solid).

On decreasing the temperature further, we observe a transformation of the PRD at approximately $T^*=2.50$. The peak located around 1 splits at lower temperatures, with one peak located at 0.92 and the second one at 1.03. This is the signature of a rectangular or quasihexagonal order in the plane perpendicular to the columns, with a distortion of 0.87. This was not seen by Bates and Luckhurst [17], since they stopped their investigations at a higher temperature. The signature of the latter transition in the other observables, such as enthalpy (Fig. 3, closed circles) or volume, for instance, is very weak and therefore difficult to observe. Nevertheless, the structural properties show clearly a change in the molecular arrangement of the system.

The first peak at 0.92 is also the signature of an interdigitation of the columns. This effect has been seen by Emerson *et al.* [16] but they attributed it to a density effect, while in our case it only comes from a decrease in the temperature.

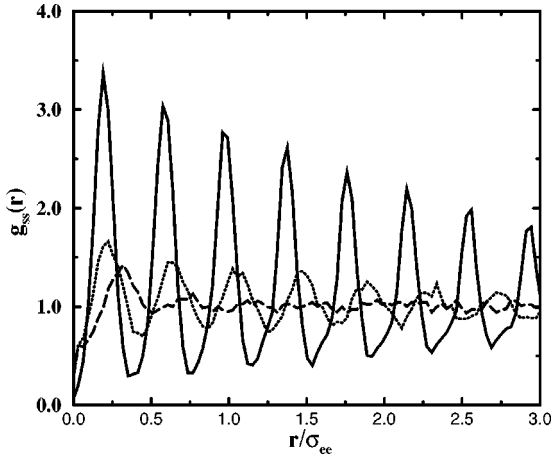

FIG. 2. Second-shell radial distribution (see text for definition) for three different temperatures : $T^*=3.20$ (long dashed) nematic phase, $T^*=2.80$ (dotted) columnar phase, and $T^*=1.40$ (solid) rectangular phase.

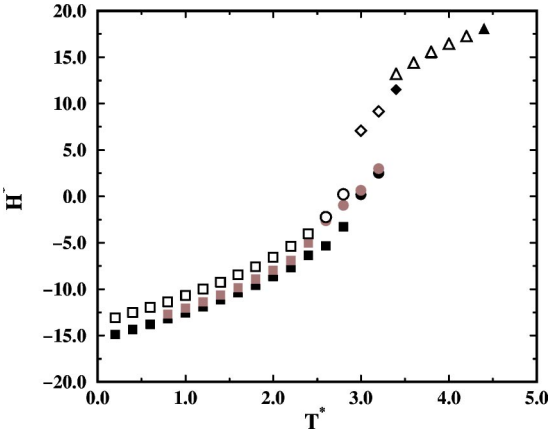

FIG. 3. Enthalpy as a function of temperature for three different runs: cooling from the high temperature end (open symbols), heating from the low temperature end (black symbols), and cooling back from an intermediate temperature reached by heating from initial perfect ordered structure (gray symbols). The symbols stand for (△) isotropic, (◇) nematic, (○) columnar, and (□) crystalline phases. For further details, see text.

One should be careful about the direct comparison with Emerson's work since the potential has been slightly changed in that work.

To check the correlations between columns, and especially the interdigitation, we introduce a new correlation function that we call second-shell radial distribution (SSRD) function and define it as

$$g_{ss}(r)=\frac{V}{N^2\pi(r_e^2-r_i^2)}\left\langle \sum_i \sum_{j\neq i} \delta(r-|\mathbf{r}_{ij}\cdot\hat{\mathbf{u}}_i|)\right\rangle, \quad (11)$$

where r_e and r_i are, respectively, the external and internal radii of a cylindrical shell on which we perform the computation. In practice, we consider all the molecules j with a radial distance to the central atom i greater than $r_i=0.5\sigma_0$ and less than $r_e=1.5\sigma_0$, and build the histogram of the $|\mathbf{r}_{ij}\cdot\hat{\mathbf{u}}_i|$ distances.

In Fig. 2, we show the SSRD for three temperatures corresponding to the nematic phase, the columnar phase found by Bates *et al.* and the new low temperature phase. In the nematic phase, the SSRD presents little structure, mainly a single peak at about $r^*=0.32$. When decreasing the temperature and crossing the N-Col$_h$ transition line, the SSRD shows seven peaks for r^* ranging from 0 to 3.

On decreasing the temperature again, the structure of the SSRD becomes more and more pronounced. At the lowest temperature, the position of the maxima is periodic with a period equal to 0.196 which is half the distance between two discotic modecules within a column.

We could conclude that at about $T^*=2.50$ the system goes from a columnar hexagonal phase to a crystalline centered orthorhombic phase. The latter one is built with two atoms per unit cell, one located at (0,0,0) and the second one in the middle of the unit cell at (1/2,1/2,1/2) in reduced units. The lattice parameters are $a=0.87$, $b=1.01$, and $c=0.39$.

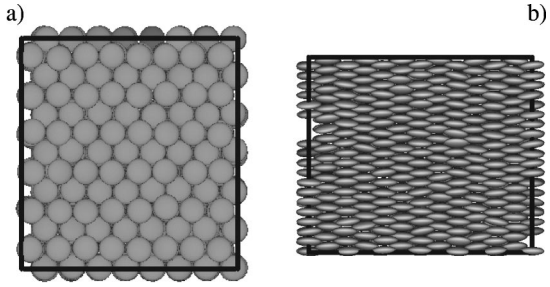

FIG. 4. View of columns from top (a) and side (b) at $T^*=1.80$ and $P^*=50$ in the crystal phase. (b) See correlations between columns.

Starting from this assumption, we build a perfect orthorhombic crystal at 0 K. We let it relax at a very low temperature $T^*=0.2$ and then heat it up to the isotropic phase at constant pressure.

Figure 3 shows the evolution of the enthalpy during heating as a function of temperature. One can clearly see three transitions. At $T^*=2.90$, the system goes from the orthorhombic phase to a new phase. As shown in snapshots of Figs. 4 and 5, this phase shows an hexagonal symmetry. At $T^*=3.30$, the system reaches the nematic phase and eventually the isotropic one at $T^*=3.50$.

One should remark that the enthalpy of the perfect orthorhombic phase is lower than that of the orthorhombic phase obtained by cooling an isotropic phase as done previously (Fig. 3). All the transition temperatures are shifted to higher values and we then observe a hysteresis. During the heating process, the hexagonal phase is mechanically less stable than during the cooling. We find an hexagonal phase over a temperature range of 0.4 against 0.6 on cooling. This effect is even more pronounced for the nematic phase. This would suggest that both triple points Cr-Col$_h$-I and Col$_h$-N-I are shifted to higher temperatures by heating, in comparison with the cooling procedure. Nevertheless, the enthalpy curve obtained during the heating seems to overlap reasonably well with the one obtained during the cooling.

To understand the difference of enthalpy measure between the cooling and the heating procedures, we perform an additional series of simulations on cooling, starting from an initial configuration of the Col$_h$ phase at $T^*=3.2$, recorded during the heating procedure mentioned above. The enthalpy measures during this cooling are represented as gray symbols

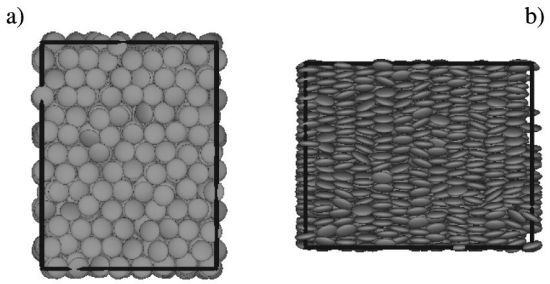

FIG. 5. View of columns from top (a) and side (b) at $T^*=3.00$ and $P^*=50$ in the columnar phase. In (b), columns are quite independent of each other.

in Fig. 3. The transition Col_h-Cr takes place at $T^*=2.5$, i.e., the same temperature observed when cooling the system all the way from the isotropic phase. We note again that the enthalpy of the crystal phase is slightly higher than the corresponding value when heating the initially perfect crystal, but the difference is definitely smaller with respect to the cooling procedure starting from the isotropic phase. From these observations, we suggest that these enthalpy differences are mainly due to the number of defects present in the sample. By cooling an isotropic configuration, one can expect many more defects in the structure than by cooling a hexagonal configuration, where the positions of the discotic molecules form a 2D hexagonal structure without defects, as it results from the melting of a perfect crystal structure. This could explain the nonreversibility of both the cooling and heating procedures.

To characterize the structure of the different phases and in particular the evolution from the hexagonal liquid crystal to the orthorhombic crystal phase, we compute the static structure factor

$$S(\mathbf{q})=\frac{1}{N}\left\langle \left| \sum_j \exp(i\mathbf{q}\cdot\mathbf{r}_j)\right|^2 \right\rangle, \tag{12}$$

where the components q_α of $\mathbf{q}$ are written as $2\pi n_\alpha/L_\alpha$ with L_α the box length in the direction α and n_α an integer.

We compute $S(q)$ for two subsets of q vectors, either orthogonal or parallel to the column's directions. At higher temperature, in the nematic phase, we define the two subsets of q vectors, either orthogonal or parallel to the nematic's director orientation. Note that the orientation of the nematic's director and the column's axes are equivalent in the Col_h and Cr phases, as the disks are standing perpendicularly to the columns axes. The analysis of the hexagonal-orthorhombic transition qualitatively gives the same results on heating or cooling. Nevertheless, due to the defects, the peaks in the columnar phases are broader on cooling than on heating. We present here the analysis done on heating.

At $q^*/2\pi$ inferior to 1.5, $S(\mathbf{q})$ computed with a set of q vectors orthogonal to the columns gives two δ functions for the orthorhombic phase ($T^*<2.50$) corresponding to the lattice parameters mentioned above and only one in the hexagonal phase (Fig. 6). This is a clear signature of a structural change from rectangular to hexagonal for the columns lateral packing. At higher temperatures ($T^*>3.20$), $S(q)$ does not show a very well-defined structure. Even if the orientational order is still present in the nematic phase, the translational one is clearly established only on short distances in the plane perpendicular to the orientation of the nematic's director.

We next compute $S(\mathbf{q})$ with a set of q vectors parallel to the columns. Figure 7 shows the results obtained for the orthorhombic and hexagonal phases. With this measurement, we check the correlations within and between columns. The parallel structure factor for the orthorhombic phase shows a δ peak corresponding to $c/2$ distances. Due to extinction rules (the sum of the three n_α integers should be even to allow a Bragg peak), the peak corresponding to c distances does not appear. This is a clear signature of a crystalline phase. For the hexagonal phase, $S(q)$ shows three broad peaks located at $1/c$, $2/c$, and $3/c$ related to intracolumn correlations. The correlations between different columns are weak, as can be seen in the snapshot of Fig. 5.

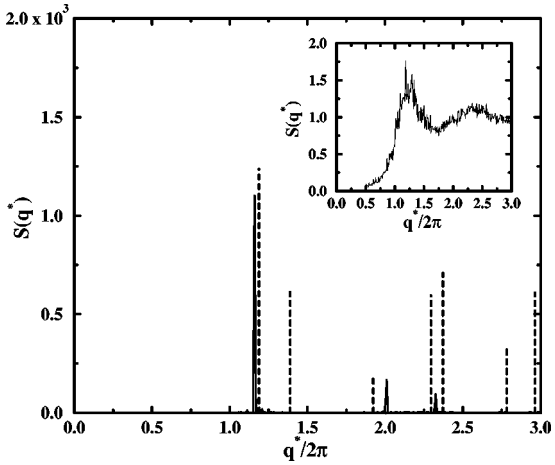

FIG. 6. Structure factor for $\mathbf{q}$ in the plane perpendicular to the columns (2D powder average) at fixed pressure $P^*=50$ and three different temperatures: $T^*=0.60$ (Cr) (dash line), $T^*=3.00$ (Col_h) (solid line), and $T^*=3.60$ (N) (inset).

To complete the analysis of these phases, we also compute the mean square displacement within (Fig. 8) and perpendicular (Fig. 9) to the columns at low temperatures. In the nematic and isotropic phase, we compute the mean square displacements along and perpendicular to the direction given by the mean orientation of the molecules.

If $\langle \Delta r^2\rangle_c$ and $\langle \Delta r^2\rangle_p$ denote the diffusion within and perpendicular to the columns, respectively, they are given by

$$\langle \Delta r^2\rangle_c=\left\langle \frac{1}{N}\sum_i \{[\delta\mathbf{r}_i(m+n)\cdot\hat{\mathbf{n}}]\}^2 \right\rangle_n \tag{13}$$

and

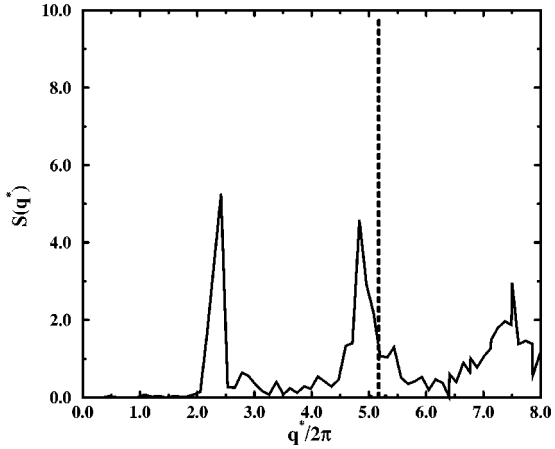

FIG. 7. Structure factor for $\mathbf{q}$ parallel to the columns at fixed pressure $P^*=50$ and two different temperatures: $T^*=0.60$ (Cr) (dashed—intensity divided by 20) and $T^*=3.00$ (Col_h) (solid).

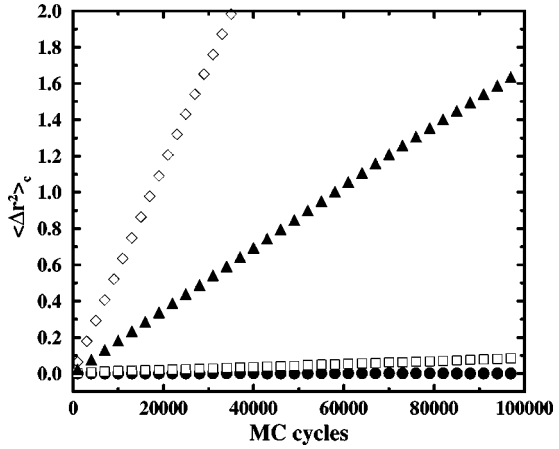

FIG. 8. Mean square displacement within the columns (or along mean molecular orientation) at several temperatures and fixed pressure $P^*=50$. From top to bottom: $T^*=4.00$ (I) ($\diamond$), $T^*=3.40$ (N) ($\blacktriangle$), $T^*=3.00$ (Col_h) ($\square$), $T^*=2.60$, and $T^*=1.00$ (Cr) ($\bullet$). The last two curves are superposed.

$$\langle \Delta r^2 \rangle_p = \left\langle \frac{1}{2N} \sum_i \left| \delta \mathbf{r}_i(m+n) - [\delta \mathbf{r}_i(m+n) \cdot \hat{\mathbf{n}}] \hat{\mathbf{n}} \right|^2 \right\rangle_n , \tag{14}$$

with $\delta \mathbf{r}_i(m+n) = \mathbf{r}_i(m+n) - \mathbf{r}_i(n)$ the displacement of the center of the mass of disk i between two MC cycles labeled by n and m. The vector $\hat{\mathbf{n}}$ is the vector giving either the direction of the columns or the mean orientation of the disks, depending on the temperature.

At high temperatures $T^*=4.00$ (I), both mean square displacements are equivalent. There is no specific direction, they are all equivalent as expected for an isotropic phase. At lower temperatures, both mean square displacements are not equivalent. In the nematic phase ($T^*=3.40$), the discotic molecules diffuse over larger distances in the plane perpendicular to the nematic's director orientation than along it. At

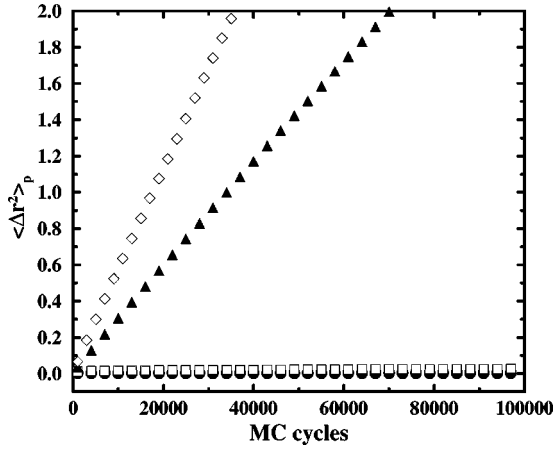

FIG. 9. Mean square displacement in a direction perpendicular to the columns (or mean molecular orientation) at several temperatures and fixed pressure $P^*=50$. From top to bottom: $T^*=4.00$ (I) ($\diamond$), $T^*=3.40$ (N) ($\blacktriangle$), $T^*=3.00$ (Col_h) ($\square$), $T^*=2.60$, and $T^*=1.00$ (Cr) ($\bullet$). The last two curves are superposed.

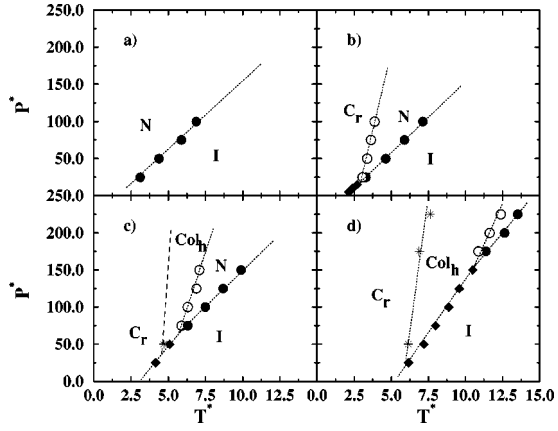

FIG. 10. Phase diagrams for several κ' parameters (see text for definition): 0.8 (a), 0.5 (b), 0.2 (c), and 0.1 (d). The symbols I stands for isotropic phase, N stands for nematic phase, Col_h stands for hexagonal columnar phase, and Cr stands for crystal. The lines are guides to the eye.

$T^*=3.00$ (Col_h), a residual diffusion is still present within the columns (even if it is weak) but it is frozen perpendicular to them. At $T^*=1.00$ (orthorhombic phase), there is no diffusion neither in nor between columns. This is another indication that the hexagonal phase is liquid crystalline, whereas the rectangular phase is crystalline.

B. Phase diagrams at $\kappa=0.2$ and κ' variable

In this section, we present the results obtained for different κ' values, keeping κ constant and equal to 0.2. This latter value is representative, for instance, of a hexaazatrinaphtalene discotic molecule [27], while κ equal to 0.345 holds for a triphenylene one [28].

Starting with a low energy anisotropy, Fig. 10(a) shows the phase diagram corresponding to κ' equal to 0.8. In the range of pressures investigated in this study, we do not find any columnar phase. Following the enthalpy at fixed pressure when decreasing temperature from 10 to 0, we observe the I-N transition and below that transition no sign of another transition. It is possible that, at sufficient low T^*, the nematic phase is metastable. At higher pressure, it is possible that a lower enthalpy phase becomes accessible, in particular, we could expect the presence of a crystalline phase.

Decreasing the κ' parameter while keeping constant κ, i.e., keeping the same shape and favoring the ff configuration against the ee one, changes the phase diagram and in particular allows the presence of an ordered phase at low pressure and temperature. This is illustrated in Fig. 10(b), where we fix κ' to 0.5. With this value, we observe three phases: the isotropic and nematic ones (already observed at higher κ') and a crystalline phase, and therefore a triple point Cr-N-I. We do not observe a columnar phase yet. The ee interactions are still too strong (in comparison with ff interactions) to decouple the correlations in the plane perpendicular to the columns and those along the columns. In other words the correlations between columns are so strong than they lead to the formation of a crystal.

We then further decrease κ' to 0.2 in order to reduce the influence of the *ee* interactions and to build columns. Figure 10(c) shows the phase diagram for this couple of parameters. We observe two triple points Cr-Col$_h$-*I* and Col$_h$-*N*-*I*. In comparison to the previously adopted κ' parameters, we observe an additional columnar phase lying between the crystalline and nematic phases. At sufficient high pressure, the system shows the following sequence of phases: crystal, columnar mesophase, nematic, and isotropic phase from low to high temperatures. Below the triple point pressure of about $P_t^*=40$, the columnar phase disappears at all temperatures. We also observe a triple point pressure of $P_t^*=65$, below which the nematic phase is not observed. For this choice of κ' parameter, the *ee* interactions are weak enough (compared to *ff* interactions) to allow for the formation of columns in a range of pressure and temperature.

To complete our study of the influence of the energy anisotropies, we further decrease κ' to 0.1. With this value, we strongly favor the *ff* interactions. As shown in Fig. 10(d), the system builds a columnar phase for a large range of pressures and temperatures. Nevertheless, we still observe two triple points corresponding to the Cr-Col$_h$-*I* and Col$_h$-*N*-*I* coexistences. The latter one is located at $P_t^*=150$ and $T_t^*=10.5$. The nematic domain is obtained for high pressures and temperatures, the strong *ff* attractions lead to the formation of columns (even at high temperatures) and an orthorhombic crystal (when decreasing the temperature).

In the P^*-T^* diagram, one can also remark that the slope and the absolute position of the *I*-*N* transition line change only slightly with κ' decreasing from 0.8 to 0.1 (Fig. 10). We find by fitting from the phase diagram a value of dP^*/dT^* ranging from 19.50 ± 1.01 to 23.29 ± 1.36, and also find by computing the Clapeyron's equation a value ranging from 19.60 ± 4.05 to 25.25 ± 5.00. These two sets of values are in fair agreement and differ from the values obtained for $\kappa=0.345$ (see Sec. III A). These results seem to indicate that the *I*-*N* transition is more driven by geometrical aspects than by energetic ones. This is not the case for the *N*-Col$_h$ one. Its slope dramatically changes with dP^*/dT^* decreasing from 57.69 ± 5.14 to 33.30 ± 5.33 when we decrease κ' from 0.2 to 0.1. The same observation holds for the Col$_h$-Cr transition, even if it is harder to quantify, the transition being too weak (see Fig. 3).

We also discuss the influence of the shape anisotropy on the phase diagram by comparing the two cases ($\kappa=0.2$, $\kappa'=0.2$) and ($\kappa=0.345$, $\kappa'=0.2$). We qualitatively find the same phase diagram for both κ values, see Fig. 10(c) and Ref. [17]. In particular, with κ equal to 0.345, we also find a triple point Col$_h$-*N*-*I* located at $P_t^*=10$ and $T_t^*=1.8$ (for $\kappa=0.2$, see above). Comparing with Fig. 10(c), we observe that by reducing the shape ratio (from 0.345 to 0.2), the Col$_h$-*N*-*I* triple point shifts to larger pressures and temperatures, P_t^* being multiplied by a factor 5.5 and T_t^* by a factor 3.

Coussaert and Baus [19] have theoretically studied the influence of the shape ratio on the phase diagram of a Gay-Berne system and we qualitatively find the same trends. The evolution of the transition lines with κ is similar, lowering the shape anisotropy leads to a reduction of the nematic domain. Nevertheless, contrary to them, we find a significant shift of the triple point when we change κ. This discrepancy on the size of the effect could be due to the approximations made in the theory. It would be interesting to perform density-functional theory calculations with κ, κ' parameters in the range explored here.

IV. CONCLUSION

We have presented a Monte Carlo study of the phase diagram of Gay-Berne discotic molecules. We have first reinvestigated the phase diagram for a $\kappa=0.345$ and $\kappa'=0.2$ system. As found by Bates and Luckhurst [17], we have obtained the same sequence: isotropic, nematic, and hexagonal columnar phases. We have additionally found an orthorhombic crystalline phase at low temperature where the discotic molecules are strongly interdigitated. In a second step, we have fixed the shape parameter and let the ratio of face-to-face over edge-to-edge energy wells vary. We have thus described a set of molecules that are weakly or strongly anisotropic from an energetic point of view. At low anisotropy (κ' close to 1), we have only observed two phases: isotropic and nematic. At intermediate κ' values (0.5), we have moreover observed an additional orthorhombic crystalline phase at low temperature. At low κ' (strong anisotropy), the phase diagram shows an hexagonal columnar phase lying between the nematic and the orthorhombic phase. We thus observe that, for discotic Gay-Berne molecules, the energy anisotropy needs to be added to shape anisotropy in order to stabilize the columnar phase. We have also shown that the triple points strongly shift with the value of κ'. Moreover, as already noticed by Coussaert and Baus [19], the nematic domain is strongly dependent on the κ value. Decreasing the latter leads to a wider (in temperature) nematic domain.

ACKNOWLEDGMENTS

We are grateful to the Communauté Française de Belgique for its financial support (ARC Grant No. 00/05-257), and we would like to thank T. Coussaert, M. Baus, I.R. Gearba, M. Lehmann, and Y.H. Geerts for fruitful and exciting discussions.

[1] S. Chandrasekhar, B.K. Sadashiva, and K.A. Suresh, Pramana **9**, 471 (1977).

[2] D. Haarer, D. Adam, J. Simmerer, F. Closs, D. Funhoff, L. Haeussling, K. Siemensmeyer, H. Ringsdorf, and P. Schuhmacher, Mol. Cryst. Liq. Cryst. Sci. Technol., Sect. A **252-253**, 155 (1994); J. Simmerer, B. Glüsen, W. Paulus, A. Kettner, P. Schuhmacher, A. Adam, K.-H. Etzbach, K. Siemensmeyer, J.H. Wendorff, H. Ringsdorf and D. Haarer, Adv. Mater. **8**, 815 (1996).

[3] J. Wright, P. Roisin, G.P. Rigby, M.J. Cook, and S.C. Thorpe,

Sens. Actuators B **13-14**, 276 (1993); A. Cole, R. McIlroy, S.C. Thorpe, M.J. Cook, J. Mc Murdo, and A.K. Ray, *ibid.* **13-14**, 416 (1993).
[4] P.H.J. Kouwer, W.F. Jager, W.J. Mijs, and S.J. Picken, Macromolecules **35**, 4322 (2002).
[5] N.H. Tinh, H. Gasparoux, and C. Destrade, Mol. Cryst. Liq. Cryst. **68**, 101 (1981); C. Destrade, N.H. Tinh, H. Gasparoux, J. Malthete, and A.M. Levelut, *ibid.* **71**, 111 (1981).
[6] T.J. Phillips, J.C. Jones, and D.G. McDonnell, Liq. Cryst. **15**, 203 (1993).
[7] P. Hindmarsh, M. Hird, P. Styring, and J.W. Goodby, J. Mater. Chem. **3**, 1117 (1993).
[8] D.S. Shankar Rao, V.K. Gupta, S. Krishna Prasad, M. Manickam, and S. Kumar, Mol. Cryst. Liq. Cryst. **319**, 193 (1998).
[9] Y. Maeda and Y. Shimidzu, Liq. Cryst. **26**, 1067 (1999).
[10] Y. Maeda, D.S. Shankar Rao, S. Krishna Prasad, S. Chandrasekhar, and Sandeep Kumar, Liq. Cryst. **28**, 1679 (2001).
[11] R. Eppenga and D. Frenkel, Mol. Phys. **52**, 1303 (1984).
[12] D. Frenkel and B.M. Mulder, Mol. Phys. **55**, 1171 (1985); B.M. Mulder and D. Frenkel, *ibid.* **55**, 1193 (1985).
[13] M.P. Allen, Phys. Rev. Lett. **65**, 2881 (1990).
[14] J.A.C. Veerman and D. Frenkel, Phys. Rev. A **45**, 5632 (1992).
[15] G. Gay and B.J. Berne, J. Chem. Phys. **74**, 3316 (1981).
[16] A.P.J. Emerson, G.R. Luckhurst, and S.G. Whatling, Mol. Phys. **82**, 113 (1994).
[17] M.A. Bates and G.R. Luckhurst, J. Chem. Phys. **104**, 6696 (1996).
[18] H. Zewdie, Phys. Rev. E **57**, 1793 (1998).
[19] T. Coussaert and M. Baus, J. Chem. Phys. **116**, 7744 (2002).
[20] J.T. Brown, M.P. Allen, and M. Warren, J. Phys.: Condens. Matter **8**, 9433 (1996); E. de Miguel, E.M. del Río, J.T. Brown, and M.P. Allen, J. Chem. Phys. **105**, 4234 (1996).
[21] R. Berardi, A.P.J. Emerson, and C. Zannoni, J. Chem. Soc., Faraday Trans. **89**, 4069 (1993).
[22] J.T. Brown, M.P. Allen, E. Martin del Río, and E. de Miguel, Phys. Rev. E **57**, 6685 (1998).
[23] M.A. Bates, and G.R. Luckhurst, J. Chem. Phys. **110**, 7087 (1999).
[24] J.L. Billeter, A.M. Smondyrev, G.B. Loriot, and R.A. Pelcovits, Phys. Rev. E **60**, 6831 (1999).
[25] C. Bacchiocchi and C. Zannoni, Phys. Rev. E **58**, 3237 (1998).
[26] R. Berardi, S. Orlandi, and C. Zannoni, Phys. Chem. Chem. Phys. **2**, 2933 (2000).
[27] G. Kestemont, V. de Halleux, M. Lehmann, D.A. Ivanov, M. Watson, and Y.H. Geerts, Chem. Commun. (Cambridge) **20**, 2074 (2001).
[28] I. R. Gearba and M. Lehmann (private communication).